DOI: 10.1002/cbic.200800746

$^{1}H\{^{19}F\}$ NOE NMR Structural Signatures of the Insulin R_6 Hexamer: Evidence of a Capped HisB10 Site in Aryl- and Arylacryloyl-carboxylate Complexes

Donald Keidel,[b] Maria Bonaccio,[a] Nima Ghaderi,[c] Dimitri Niks,[a] Dan Borchardt,[d] and Michael F. Dunn*[a]

Although transplantation and stem cell therapies look promising, at present, type 1 (insulin-dependent) diabetics can be treated only with insulin or insulin analogues.[1,2] Hexameric insulin is widely used in pharmaceutical formulations for treatment of insulin-dependent diabetes mellitus.[3,4] The stability and dynamic properties of human insulin (HI) zinc hexamer formulations are critically influenced by allosteric effectors.[3–17] Therefore, the discovery of ligands with enhanced allosteric and/or pharmacological properties is important for the design of improved formulations.[3,4]

Insulin hexamers exhibit positive and negative cooperativity and half-of-the-sites reactivity in ligand binding.[3–17] The HI hexamer undergoes allosteric transitions among three well-characterized protein conformations, which are designated T_6, T_3R_3, and R_6.[5–17] Crystalline and precipitated T_3R_3 and R_6 hexamers are formulated as slow-release forms,[3,4] and are stabilized by the binding of allosteric ligands at two loci, the "phenolic pockets" (3 in T_3R_3 and 6 in R_6), and the "HisB10 zinc sites" (1 in T_3R_3 and, 2 in R_6).[3,4,13–16] The R-state HisB10 sites (Figure 1) bind monovalent anions (halides, pseudo halides, and carboxylates).[3,4,13–16] Binding interactions are structurally well characterized at the phenolic pockets[9–12] but not at the HisB10 sites. Each HisB10 site is formed by a three-helix bundle consisting of B-chain residues 1–9 situated around the hexamer three-fold symmetry axis, to create 12 Å deep amphipathic cavities.[4,9–12] These cavities extend from the protein surface to the HisB10 Zn^{II} (Figure 1). Monoanions bind in these cavities and coordinate to Zn^{II} and give pseudotetrahedral Zn^{II}–$(His)_3$-X^- complexes ($X^- = Cl^-$ or SCN^-),[9–16,18–21] (Figure 1) or 5-coordinate complexes with carboxylates.[12–14,19–21] This $^{1}H\{^{19}F\}$ NOE study was undertaken to identify weak bonding interactions between the ligand and the cavity residues that stabilize the binding of organic carboxylates to the HisB10 zinc sites.

The binding of carboxylates to the HisB10 site has been extensively investigated in solution, and it is unambiguously established that binding involves coordination to the HisB10 zinc ions;[6,8,16,18–21] however, no X-ray structures of R-state carboxylate complexes have been published. Aromatic carboxylates make contacts with the HisB10 cavity walls that contribute substantially to the binding free energy.[3,8,19–21] The T_3R_3 and R_6 Cl^- or SCN^- complexes (Figure 1) give HisB10 sites with the anion positioned on the hexamer three-fold symmetry axis and coordinated to Zn^{II}.[9–12,22–24] The structure most relevant to this work, 1ZNJ,[22] has one HisB10 cavity of HI–R_6 that is occupied both by a Cl^- coordinated to Zn^{II} and by a phenol. The phenol ring makes contact with Cl^- and with the AsnB3, and LeuB6 sidechains in each 3-helix bundle. One PheB1 ring is within 5 Å of the phenol ring, one points away, and the third is disordered. The resorcinol-stabilized Cl^- complex (1EVR) is similar.[23] A structure with a phenolate ion coordinated to a HisB10 site was reported,[12,24] but no coordinates were deposited. The absence of X-ray structures that show details of an aromatic carboxylate bound to the HisB10 cavity of an HI complex likely is due to disorder arising from the loss of the three-fold molecular symmetry from placement of a planar ligand into the site. The planar ligand would be expected to randomly take up any

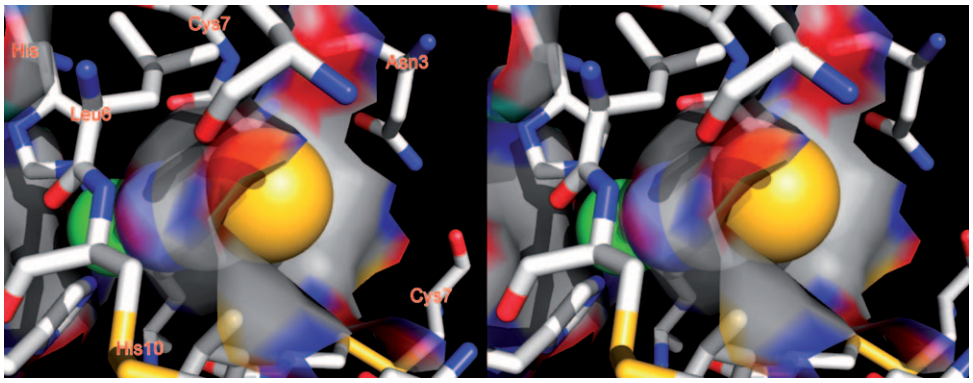

Figure 1. Stereoview of the HisB10 R_3 site with SCN^- coordinated to Zn^{II} (green). The hexamer three-fold symmetry axis (not shown) passes through Zn^{II} and the S, C, and N atoms of SCN^-. The surface depicts the HisB10 anion binding site. SCN^- (van der Waals spheres) AsnB3, LeuB6, CysB7, and HisB10 (sticks) are shown with CPK colors. The image was created by using PyMOL 1.0 and PDB structure 2TCI.[10]

[a] Dr. M. Bonaccio, D. Niks, Prof. Dr. M. F. Dunn
Department of Biochemistry, University of California at Riverside
Riverside, California 92521 (USA)
Fax: (+1) 951-827-4434
E-mail: michael.dunn@ucr.edu

[b] Dr. D. Keidel
The Scripps Research Institute, Department of Molecular Biology
La Jolla, California 92037 (USA)

[c] Dr. N. Ghaderi
Division of Chemistry and Chemical Engineering
California Institute of Technology
Pasadena, California 91125 (USA)

[d] Dr. D. Borchardt
Department of Chemistry, University of California at Riverside
Riverside, California 92521 (USA)

Supporting information for this article is available on the WWW under http://dx.doi.org/10.1002/cbic.200800746.

one of three symmetry-related positions[4,8,21] throughout the crystal lattice.

^{19}F NMR spectroscopy of fluorinated ligands complexed to protein sites can be useful for investigating protein structure–function relationships.[8,25–27] Four ligands were investigated herein, 3-trifluoromethylbenzoate (**1**), 4-trifluoromethylbenzoate (**2**), 3-trifluoromethylcinnamate (**3**), and 4-trifluoro-methylcinnamate (**4**). 1D ^1H NMR spectra and $^1H\{^{19}F\}$ NOE difference spectra of R_6 HI and the R_6 HI variant with B-chain Phe1Glu and Thr27Glu were measured at pH 8.0 in D_2O[8,26,27] at 500 MHz (viz., Figures 2 and 3). The 1D ^1H NMR spectra (Figure 2A) and the $^1H\{^{19}F\}$ NOE difference experiment (Figures 2B and 3) characterize the complexes of compound **1** formed with the [D_6]phenol-stabilized R_6 hexamers of HI (blue traces) and the HI variant (red traces). The assigned $^1H\{^{19}F\}$ NOE difference spectra for the aromatic and aliphatic regions are shown in Figures 2B and 3, respectively. Chemical shifts of protein resonances for HI–R_6 complexes with ligand **1** gave excellent agreement (±0.05 ppm) for most residues with the values that were reported for the R_6 complex with the HisB10 ligand, 3-nitro-4-hydroxybenzoate (**5**).[21] Except for differences due to the amino acid substitutions, the resonances of the HI variant complex gave similar agreement.

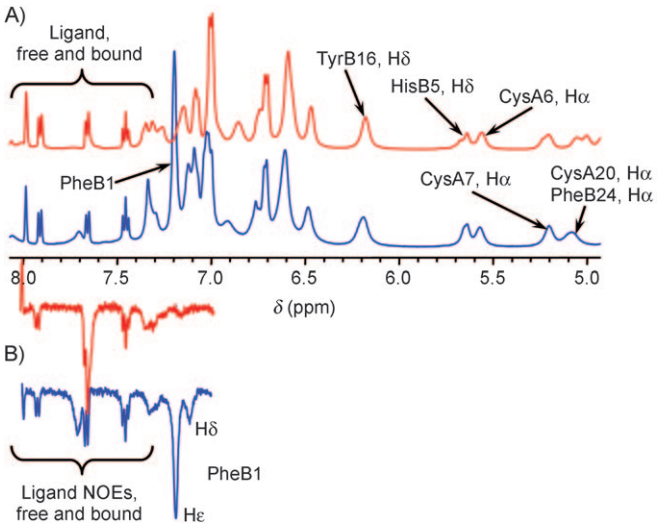

Figure 2. A) ^1H NMR spectra comparing R_6 complexes of **1** with human insulin (blue) and with the human insulin variant with B-chain Phe1Glu and Thr27Glu (red). B) Aromatic region of the $^1H\{19F\}$ NOE difference spectra for R_6 human wild-type (blue) and R_6 variant (red) complexes with **1**.

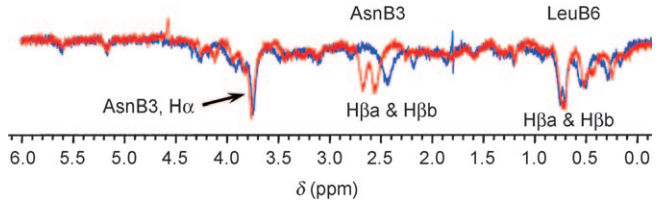

Figure 3. Aliphatic region of the $^1H\{^{19}F\}$ NOE difference spectra for R_6 human insulin (blue) and the human insulin variant (red) complexes with **1**. Spectra: average of 16000 scans, mixing time = 0.9 s, acquisition time = 2.047 s, relaxation delay = 1.5 s.

The 1D ^1H NMR spectra (Figure 2A) include peaks in the 7.3 ppm to 8.3 ppm region for free ligand (sharp) and bound ligand (broad, slightly shifted); this is consistent with moderately slow to slow exchange.[8,21] The signature protein peaks at 5.0 ppm to 6.6 ppm (Figure 2A) establish that both the HI and the variant complexes have the R_6 conformation.[13–15,18–21,28–30] The complexes with compounds **2**–**4** gave similar results (data not shown).

The $^1H\{^{19}F\}$ NOE difference spectra (Figures 2B and 3) allowed us to identify protein residues within ~5 Å of the CF_3 fluorine atoms of bound **1**. By comparison of chemical shift values with the assigned resonances of the HI–R_6 complex with **5**,[21] assignments of the strong peaks were made for the complex of HI–R_6 with **1**. The ring protons of PheB1 give resonances at 7.31 and 7.34 ppm in the complex with **5**, and the corresponding complex with Cl^- gives PheB1 resonances at 7.30 and 7.34 ppm.[21] The NOEs in Figure 2B at 7.13 and 7.20 ppm in HI are completely missing in the HI variant R_6 difference spectrum, whereas there is a good correspondence between NOEs observed in HI and in the HI variant elsewhere in the spectrum. Because the variant has PheB1 replaced by Glu, the absence of NOEs between 7.0 and 7.28 ppm in the variant must be due to the substitution of Glu for Phe; this confirms that the 7.13 and 7.20 ppm signals in the HI complex arise from NOEs between the fluorine atoms of the CF_3 group of **1** and the PheB1 Hδ and Hε atoms (slightly shifted by ligand ring current effects). The HI–R_6 complexes with compounds **2**–**4** also show strong NOE interactions at 7.28 ppm that are similar to the 7.20 ppm peak in the complex with **1**.

In the aliphatic region, the HI variant and HI–R_6 complexes with **1** give similar NOEs with chemical shifts assigned to the protons of LeuB6 and AsnB3 (Figure 3) based on the assignments for the HI complex with **5**.[21] Because the binding locus is not in question,[8,15,16,19–21] a more rigorous assignment method was not needed. Control experiments demonstrated that spin diffusion was not responsible for any of the observed NOEs (see Figures S1–S3 in the Supporting Information).

The NOEs observed between the CF_3 fluorine atoms of compounds **1**–**4** and the PheB1 rings were unexpected. In most X-ray structures of HI–R_6, the PheB1 rings extend out into solution >6 Å away from the opening to the HisB10 site. Because there are no published structures of aromatic carboxylates bound to the HisB10 site, we decided to explore the binding of ligands **1**–**4** by modeling their structures into the HisB10 site of the HI–R_6 hexamer, 1ZNJ.[22] Figure 4 shows a structural model based on the coordinates for 1ZNJ that is consistent with the observed NOEs for the HI complex with **1**. This model was generated as follows: the coordinates for Cl^- and phenol at the HisB10 site in 1ZNJ were replaced by **1**, hydrogen atoms were added to the protein, and crystallographic water, and disordered protein residues were replaced prior to simulation. Minimization was performed by using the Discover (CVFF force field) and Discover_3 (ESFF force field) modules present in the molecular modeling 3D graphical interface, Insight II.[31–34] Both water and protein objects were minimized in turn by using a Cell-Multipole summation, then the "steepest descents" minimization algorithm, and finally the Polak–Ribiere Conju-

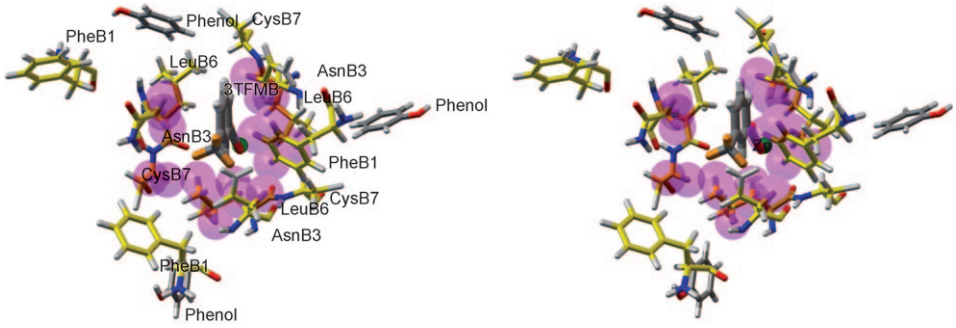

Figure 4. Stereodiagram of the energy-minimized structural model[10,16] of **1** bound to the HisB10 site of the phenol-stabilized HI R_6 hexamer as viewed from solution along the Zn–Zn axis. The HisB10 site is capped by one PheB1 residue and the three AsnB3 residues. For clarity, only the PheB1, AsnB3, LeuB6, and CysB7 residues are shown. Compound **1** and the phenols at the phenolic pockets are represented in ball and sticks with CPK coloring. Color code: all protein C atoms, yellow; F, bronze; H within 5 Å of F, magenta with transparent magenta van der Waals surfaces; all other H, white; Zn^{II}, green. The image was created by using Python Molecular Viewer.[35]

gate Gradient minimization (convergence value = 0.10).[31–34] The model (Figure 4) shows **1** coordinated to the HisB10 Zn^{II} in one of three symmetry-related positions. In this model, the H atoms of LeuB6, AsnB3, and the PheB1 ring are within 5 Å of the fluorine atoms of CF_3. Ligand exchange among the three symmetry-related positions would allow NOEs to each of the three LeuB6, AsnB3, and PheB1 residues that form the walls of the cavity.

These NOE experiments establish that the complex of **1** with HI–R_6 takes up a conformation in which the PheB1 ring protons are located within 5 Å of the fluorine atoms present on the CF_3 group. The structural model (Figure 4) predicts that **1** makes van der Waals contact with the ring of a PheB1 in a structure where this PheB1 and the AsnB3 residues cap the HisB10 anion-binding site. Structural models also were calculated for compounds **2**–**4**. These models show a similar capping of the HisB10 site (Figure S4). The model structures suggest possible strategies for the design of aromatic carboxylates as allosteric effectors to stabilize R-state HI hexamers for use in formulations to treat diabetes.

Experimental Section

Zn^{II}-free human insulin and the insulin variant with B-chain Phe1Glu and Thr27Glu were gifts from Novo Nordisk. All other chemicals were purchased from Sigma–Aldrich and used without further purification. Samples of zinc–insulin hexamers were prepared for NMR spectroscopy as was previously described,[8] by incubation of the proteins in D_2O so that the only resonances observed were from **1** and the non-exchangeable/very slowly exchanging protons of the proteins. The pulse sequence used for these experiments gave the $^1H\{^{19}F\}$ NOEs directly. Alternate scans were subtracted to leave the NOE. Consequently, only half the scans lead to accumulation of NOE signals with the other half providing a correction for T1 relaxation during the mixing time. This sequence can easily detect NOEs in the 0.1% range. The observation of NOEs was critical to this study, not their quantification; however, NOEs observed here are estimated to be in the 1–2% range.

Acknowledgements

We thank Novo Nordisk for the wild-type human and variant insulin, and for a gift to M.F.D. in support of this work.

Keywords: ^{19}F NMR · allosterism · insulin · molecular modeling · NMR spectroscopy · nuclear Overhauser effect

[1] R. S. Porter, *Merck Manual, Home Edition*, online version, **2007**, http://www.merck.com/mmhe/index.html.
[2] F. M. Ashcroft, S. J. H. Ashcroft, *Insulin. Molecular Biology to Pathology*, IRL, New York **1992**.
[3] S. Rahuel-Clermont, C. A. French, C. I. Chou, N. C. Kaarsholm, M. F. Dunn, *Biochemistry* **1997**, *36*, 5837.
[4] M. F. Dunn, *Biometals* **2005**, *18*, 295.
[5] N. C. Kaarsholm, H. C. Ko, M. F. Dunn, *Biochemistry* **1989**, *28*, 4427.
[6] M. L. Brader, M. F. Dunn, *Trends Biochem. Sci.* **1991**, *16*, 341.
[7] M. L. Brader, N. C. Kaarsholm, R. W.-K. Lee, M. F. Dunn, *Biochemistry* **1991**, *30*, 6636.
[8] M. Bonaccio N. Ghaderi, D. Borchardt, M. F. Dunn, *Biochemistry* **2005**, *44*, 7656.
[9] U. Derewenda, Z. Derewenda, E. J. Dodson, G. G. Dodson, C. D. Reynolds, G. D. Smith, C. Sparks, D. Swensen, *Nature* **1989**, *338*, 594.
[10] J. L. Whittingham, S. Chaudhuri, E. J. Dodson, P. C. E. Moody, G. G. Dodson, *Biochemistry* **1995**, *34*, 15553.
[11] E. Ciszak, G. D. Smith, *Biochemistry* **1994**, *33*, 1512.
[12] G. D. Smith, G. G. Dodson, *Biopolymers* **1992**, *32*, 441.
[13] W. E. Choi, M. L. Brader, V. Aguilar, N. C. Kaarsholm, M. F. Dunn, *Biochemistry* **1993**, *32*, 11638.
[14] M. L. Brader, N. C. Kaarsholm, R. W.-K. Lee, M. F. Dunn, *Biochemistry* **1991**, *30*, 6636.
[15] P. S. Brzovic, W. E. Choi, D. Borchardt, N. C. Kaarsholm, M. F. Dunn, *Biochemistry* **1994**, *33*, 13057.
[16] C. R. Bloom, W. E. Choi, P. S. Brzovic, J. J. Ha S.-T. Huang, N. C. Kaarsholm, M. F. Dunn, *J. Mol. Biol.* **1995**, *245*, 324.
[17] D. T. Birnbaum, S. W. Dodd, B. E. H. Saxberg, A. D. Varshavsky, J. M. Beals, *Biochemistry* **1996**, *35*, 5366.
[18] M. Roy, M. L. Brader, R. W. Lee, R. N. C. Kaarsholm, J. F. Hansen, M. F. Dunn, *J. Biol. Chem.* **1989**, *264*, 19081.
[19] M. L. Brader, N. C. Kaarsholm, S. E. Harnung, M. F. Dunn, *J. Biol. Chem.* **1997**, *272*, 1088.
[20] S. T. Huang, W. E. Choi , C. R. Bloom, M. Leuenberger, M. F. Dunn, *Biochemistry* **1997**, *36*, 9878.
[21] H. B. Olsen, M. R. Leuenberger-Fisher, W. Kadima, D. Borchardt, N. C. Kaarsholm, M. F. Dunn, *Protein Sci.* **2003**, *12*, 1902 (see the Supporting Information).
[22] M. G. W. Turkenberg, J. L. Whittingham, J. P. Turkenberg, G. G. Dodson, U. Derewenda, G. D. Smith, E. J. Dodson, A. S. Derewenda, B. Xiao, PDB ID: 1ZNJ, **1997**.
[23] G. D. Smith, E. Ciszak, L. A. Magrum, W. A. Pangborn, *Acta Crystallogr. Sect. D Biol. Crystallogr.* **2000**, *56*, 1541.
[24] G. D. Smith, G. G. Dodson, *Proteins Struct. Funct. Genet.* **1992**, *14*, 401.
[25] D. H. Gregory, J. T. Gerig, *Biopolymers* **1991**, *31*, 845.
[26] E. Y. Lau, J. T. Gerig, *Biophys. J.* **1997**, *73*, 1579.
[27] J. T. Gerig, *Magn. Reson. Chem.* **1999**, *37*, 647.
[28] D. Ferrari, J. R. Diers, D. F. Bocian, N. C. Kaarsholm, M. F. Dunn, *Biopolymers* **2001**, *62*, 249.
[29] E. Jacoby, Q. X. Hua, A. S. Stern, B. H. Frank, M. A. Weiss, *J. Mol. Biol.* **1996**, *258*, 136.

[30] X. Chang, M. M. Jørgensen, P. Bardrum, J. J. Led, *Biochemistry* **1997**, *36*, 9409.
[31] Accelrys Inc. Discover, Accelrys Inc., USA **1998**.
[32] Accelrys Inc. Discover_3, Accelrys Inc., USA **1998**.
[33] Accelrys Inc. Biopolymer, Accelrys Inc., USA **1998**.
[34] Accelrys Inc. Insight II, Accelrys Inc., USA **1998**.
[35] M. F. Sanner, *J. Mol. Graphics Model.l.* **1999**, *17*, 57–61.

Received: November 12, 2008
Published online on January 14, 2009

